



Experiment Report Form



<p><b>Experiment title:</b> Residual Stress Relaxation when VPPA Welded Aerospace Structures are Exposed to Design Limit Loads</p>	<p><b>Experiment number:</b> ME 618</p>	
<p><b>Beamline:</b></p>	<p><b>Date of experiment:</b> from: 23-07-03 to: 28-07-03</p>	<p><b>Date of report:</b> 08-03-04</p>
<p><b>Shifts:</b> 17</p>	<p><b>Local contact(s):</b> Dr. Michela Brunelli</p>	<p><i>Received at ESRF:</i></p>

**Names and affiliations of applicants (\* indicates experimentalists):**

**L. Edwards\*, S. Ganguly\*, V. Stelmukh\* and S. Pratihari\***

Dept of Materials Engineering, Open University, Walton Hall, Milton Keynes MK7 6AA

**Report:**

In the aerospace industries significant research effort has been concentrated on weight saving and innovative design options for the future generation very large aircraft [1]. Welding has been identified as one of the potential and cost effective alternative to mechanical fastening for fabrication of structural components including wing skin stringer panels. However the use of welding instead of mechanical fastening could lead to the formation of a variable distribution residual stress field with changed grain size and microstructural features. Therefore, before implementation of such process change the effect of residual stress distribution and changed microstructure on the fatigue crack propagation behaviour needs to be ascertained for damage tolerant design of safety critical aircraft structural members. In the previous experiments ( Experiment no. ME281, ME515 and ME516) we determined the residual strain distribution in the two in-plane principal strain directions for AA2024 and AA7150 used in the lower and upper wing skin stringer assemblies respectively. Two candidate weld processes, the Metal Inert Gas (MIG) and the Variable Polarity Plasma Arc (VPPA) welding processes were studied. The strain distributions in the longitudinal and transverse strain directions of the AA2024-T351 were carried out in the as-welded coupon sample of dimension 240x280x12.5mm<sup>3</sup> (VPPA welds) and 186x285x12.5mm<sup>3</sup> (MIG welds). Strains from the two principal in-plane directions were then combined with the out-of-plane (normal direction) strain measured in a neutron source and the full 3 dimensional residual stress tensor across the weld was determined[2, 3]. The stress evolution due to reduction in thickness was also determined by measuring the as-welded plate after skimming to 7mm in the through thickness direction. The AA7150 is characterised by strong texture component and utilising this feature the 3-dimensional stress tensor across the weld in the skimmed sample was determined and reported[4]. Although these data provide the very useful insight to the processes and the stress generation and distribution profile, for direct supplementation with the fatigue crack growth data it is necessary to characterise the residual stress profile on similar length scale to that of the fatigue sample. Also the change in residual stress magnitude and distribution pattern during loading provides vital input to the fatigue crack growth behaviour during testing. In this experiment the residual stress distribution pattern in machined fatigue specimens and its evolution during loading was determined.

**Sample Description**

In this experiment two types of fatigue testing specimens were studied

1. Autogeneous VPPA welded AA2024-T351 specimen of dimension  $100 \times 90 \times 7 \text{mm}^3$  in as-machined condition and after 3pt bend loading to 360MPa and released. This sample was used to determine the nucleation of fatigue cracks and growth upto 1mm.
2. Autogeneous VPPA welded AA7150-W51(Post Weld Heat Treated to T651) of dimension  $300 \times 80 \times 7 \text{mm}^3$  in as-machined condition and after subjecting to an uniaxial load of 180MPa and then releasing. This specimen is used to measure fatigue crack growth rates in long ( $>1 \text{mm}$ ) cracks.

The shown sample of VPPA welded AA2024 is for short crack characterisation and in those samples crack formation and growth up to 1mm was monitored. The VPPA welded AA7150-W51 sample was utilised to monitor crack growth through the weld. The sample shapes, dimensions and the loading mechanisms are shown in fig 1 a) & b). The principal directions measured were also shown in the figures. The welding in these samples were carried out along the rolling directions which is taken as the longitudinal direction (LD), the direction across the weld is taken as the transverse direction (TD) and the through thickness direction is taken as the normal direction (ND).

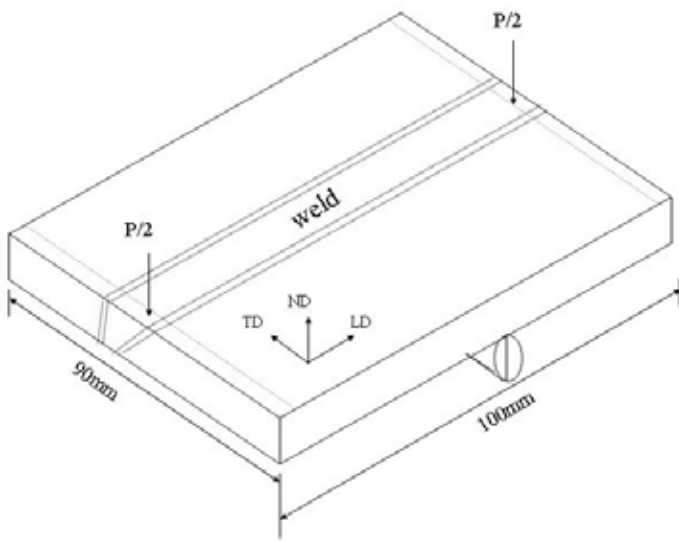


Fig 1a) Short crack growth sample VPPA welded AA2024-T351

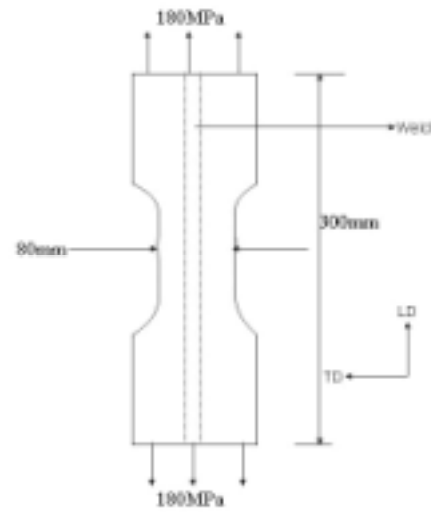


Fig 1b) Long crack growth sample VPPA welded AA7150-PWHT to T651

## Experimental Details

For both the samples the 3-dimensional surface stress tensor was determined in as machined condition and after application of the maximum design load in the laboratory to determine stress shakedown. The AA2024 is not highly textured and so the 311 reflection was used to determine the lattice spacing. The stress free reference values were obtained from measurement of a do comb sample of dimension  $3 \times 3 \times 12 \text{mm}^3$  and of insufficient constraint to hold an internal residual stress field. The AA7150 on the other hand is characterised by a high degree of preferred orientation and different reflections had to be used to determine the strain along the different principal axes. For measuring the longitudinal direction the 422 reflection was used while for measurement of transverse and normal directions 222 and 440 reflections were used respectively. However, use of the same reflections during measurement of the stress free reference comb sample eliminated the possibility of undue accounting of intergranular strains. Synchrotron radiation is ideal to measure in-plane strain directions [5] while the out-of-plane strain direction are not commonly measured by this technique since that would lead to a high path length ( $2 \times \text{depth} / \sin\theta$ ) and the intensity of the diffracted beam will not be measurable. However, in the experiment all three directions were measured since stresses were required only 0.5mm from the surface and the path length of about 8.5mm was just attainable using an incident beam of energy 45KeV. Synchrotron X-rays are better suited to determine the surface strain. In ID31 the detectors are preceded by analyser crystals which stringently defines the angle of diffraction, therefore there is no possibility of peak shift due to gauge aberration during measurement of surface strain profile. The strain calculated for all the three principal directions was converted to stress with the approximation of Hooke's law as shown in equation 1.

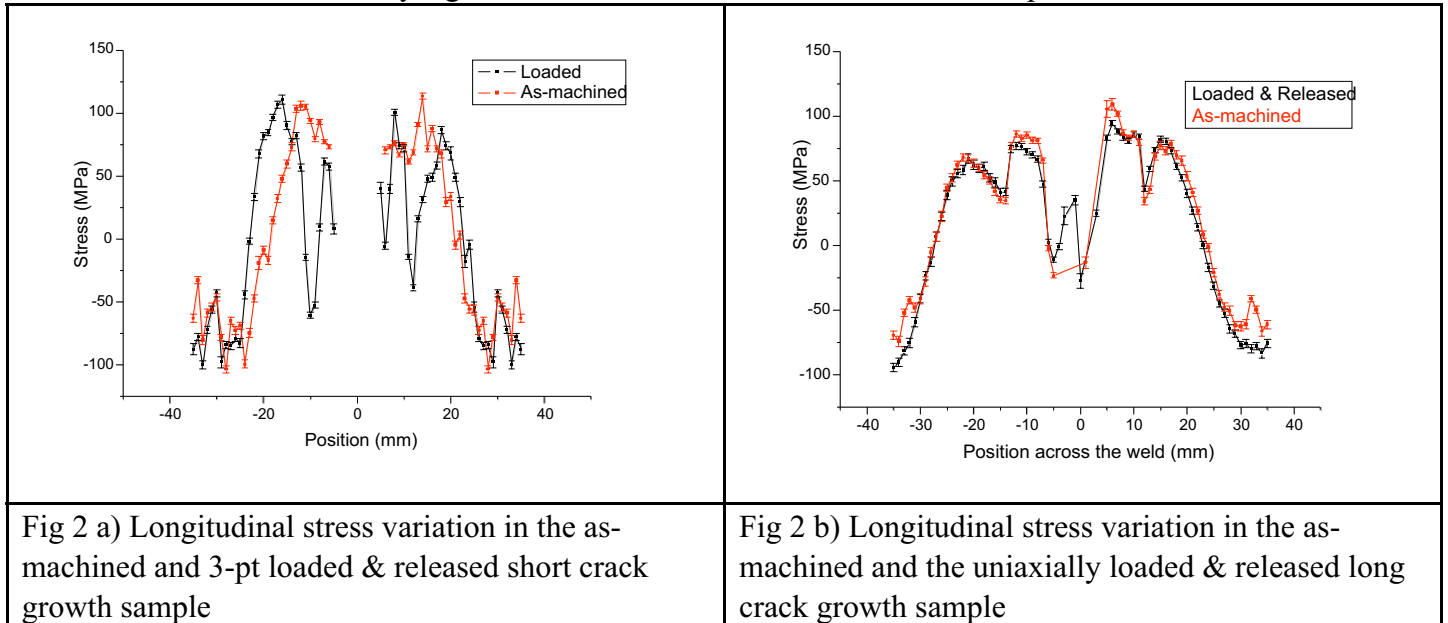
$$\sigma_{ii} = \frac{E}{1+\nu} \epsilon_{ii} + \frac{E\nu}{(1+\nu)(1-2\nu)} \epsilon_{kk} \text{-----(1)}$$

where E is the elastic modulus, and  $\nu$  is the poisson's ratio and  $\epsilon_{kk} = \epsilon_{LD} + \epsilon_{TD} + \epsilon_{ND}$

## Results

The near surface stress variation in the longitudinal direction for the short crack growth and the long crack characterisation samples are shown in fig 2 a) & b).

It can be seen from the figures that in the short crack growth sample which was 3-pt bend loaded to the maximum design load, the peak stress locations on either side of the weld are shifted to the far side of the weld by 8mm. The specimen for long crack characterisation on application of its, smaller maximum design load did not show any significant variation from the as-machined sample.



The higher magnitude of the load applied in the 3-pt bend specimen to study small crack growth causes the residual stress peaks to shift. This is because the peak load locations relaxes at the high load as it is plastically deformed and the inhomogeneous plastic deformation on the surface along the weld line shifts the maximum stress peak. However, these measurements quantify the extent of peak shift and it is interesting to note that small crack nucleation was most prevalent in the areas of high residual stress.

The lower (elastic) level of uniaxial loading in the long crack specimen did not show any redistribution on loading. However, there was still a strong correlation between the fatigue crack growth rate and the local residual stress variation.[6].

These experimental results have been compared with fatigue testing data and are yielding very encouraging results in terms of understanding the mechanism of fatigue crack generation and growth under the variable residual stress field[7]

## Reference:

1. Heinz, A., et al., *Recent developments in aluminium alloys for aerospace application*. Materials Science and Engineering, 2000, A280: pp.102-107.
2. Ganguly, S., et al., *Use of neutron and synchrotron X-ray diffraction for non-destructive evaluation of weld residual stresses in aluminium alloy*. In Press, J Neutron Research, 2004.
3. Stelmukh, V., et al., *Weld Stress Mapping Using Neutron and Synchrotron X-ray Diffraction*. Materials Science Forum, 2002 (404/407): pp. 599-604.
4. Stelmukh, V., L. Edwards, and S. Ganguly, *Full Stress Tensor Determination in a Textured Aerospace Aluminium Alloy Plate*. Textures and Microstructures, 2003. 35(3/4): p. 175-183.
5. Webster, P.J. and P.J. Withers, *Neutron & synchrotron X-ray strain scanning*. Strain, 2001, 37: p. 19.
6. Lin, J., et al., *The effects of residual stress and HAZ on fatigue crack growth*. Proc Fatigue 2003:, ISBN 0 9544368 0 6, 2003.
7. Lefebvre, F., Ph.D Thesis, *Micromechanical assessment of fatigue in airframe fusion welds*, in School of Engineering Sciences. 2003, Univ. Southampton.